analytical chemistry

ARTICLE

pubs.acs.org/ac

Responsive Polymers-Based Dual Fluorescent Chemosensors for Zn^{2+} Ions and Temperatures Working in Purely Aqueous Media

Tao Liu and Shiyong Liu*

CAS Key Laboratory of Soft Matter Chemistry, Department of Polymer Science and Engineering, Hefei National Laboratory for Physical Sciences at the Microscale, University of Science and Technology of China, Hefei, Anhui 230026, China

Supporting Information

ABSTRACT: We report on the fabrication of responsive double hydrophilic block copolymers (DHBCs)-based dual fluorescent chemosensors for Zn^{2+} ions and temperatures and investigate the effects of thermo-induced micellization and detection conditions on the probing sensitivity and binding reversibility of Zn^{2+} ions. A novel quinoline-based polarity-sensitive and Zn^{2+}-recognizing fluorescent monomer (ZQMA, **6**) was synthesized at first. Well-defined DHBCs bearing quinoline-based Zn^{2+}-recognizing moieties (ZQMA) in the thermoresponsive block, PEG-*b*-P(MEO_2MA-*co*-OEGMA-*co*-ZQMA), were synthesized via reversible addition−fragmentation chain transfer (RAFT) polymerization of 2-(2-methoxyethoxy)ethyl methacrylate (MEO_2MA), oligo(ethylene glycol) monomethyl ether methacrylate (OEGMA), and ZQMA in the presence of PEG-based macroRAFT agent. The OEGMA contents in the thermoresponsive block varied in the range of 0−12.0 mol % to tune their lower critical solution temperatures (LCSTs). At 20 °C, almost nonfluorescent PEG-*b*-P(MEO_2MA-*co*-ZQMA) molecularly dissolved in water and can selectively bind with Zn^{2+} ions over other common metal ions, leading to prominent fluorescence enhancement due to the coordination of ZQMA with Zn^{2+}. At a polymer concentration of 0.2 g/L, the Zn^{2+} detection limit can be down to ∼3.0 nM. PEG-*b*-P(MEO_2MA-*co*-ZQMA) self-assembles into micelles possessing P(MEO_2MA-*co*-ZQMA) cores and well-solvated PEG coronas upon heating to above the LCST, and the fluorescence intensity exhibit ∼6.0-fold increase due to the fact that ZQMA moieties are now located in a more hydrophobic microenvironment. Compared to the unimer state at 20 °C, although PEG-*b*-P(MEO_2MA-*co*-ZQMA) micelles possess a slightly decreased detection limit for Zn^{2+} (∼14 nM), reversible binding between ZQMA moieties and Zn^{2+} ions at 37 °C can be achieved, as evidenced by the on/off switching of fluorescence emission via the sequential addition of Zn^{2+} and EDTA. In vitro fluorescence imaging studies suggested that the micelles can effectively enter into living cells and sensitively respond to Zn^{2+} ions. This work represents the first example of a purely aqueous-based polymeric Zn^{2+} sensing system by integrating the well-developed small molecule Zn^{2+}-sensing moieties with stimuli-responsive DHBCs.

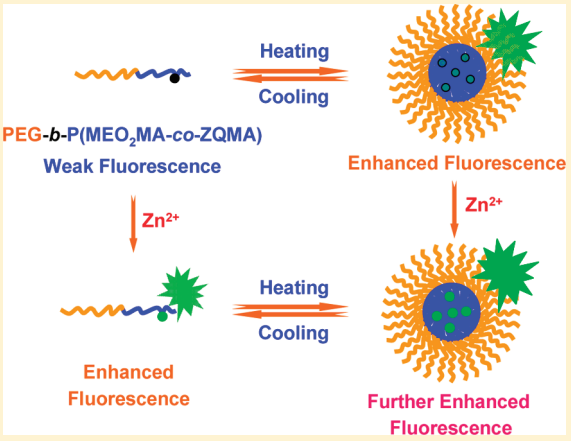

Zinc, as the second most abundant transition metal in the human body,[1] plays an indispensable role in various biological processes such as gene transcription, regulation of metalloenzymes, cell apoptosis, neural signal transmission, and insulin secretion, to name a few.[2−6] Moreover, the deviation of Zn^{2+} concentrations from normal levels might also be associated with a variety of diseases including Alzheimer's disease, diabetes, epilepsy, and infantile diarrhea.[7,8] According to the World Health Organization, more than 40% of the children in Africa and Asia encounter the stunted growth problem presumably due to the limited uptake of zinc.[9] Generally, the total concentration of Zn^{2+} ions in different types of cells is quite varied, ranging from the nanomolar level to ∼0.3 mM.[2,10] Thus, the highly sensitive, selective, and reversible detection and imaging of Zn^{2+} ions in living cells, tissues, and organs is of vital importance. Unfortunately, unlike other biorelevant transition metal ions such as Fe^{2+}, Fe^{3+}, Mn^{2+}, and Cu^{2+} ions, Zn^{2+} do not give any spectroscopic or magnetic signals due to its $3d^{10}4s^0$ electronic configuration.[1] In this context, the fluorometric detection of Zn^{2+} has been quite appealing considering its high sensitivity, noninvasiveness, high spatial resolution, and the capability of real-time monitoring.[9,11−16]

In the past few decades, a variety of fluorescent Zn^{2+} probes have been developed based on small molecules (such as derivatives of anthracene,[17−21] fluorescein,[22−36] coumarin,[37−42] 1,8-naphthalimide,[43−47] 7-nitro-1,2,3-benzoxadiazole,[48,49] boron dipyrromethene,[50−52] cyanine,[53,54] rhodamine,[55−58] and quinoline[59−73]), peptides,[74−76] proteins,[77,78] and nanoparticles.[79,80]

Received: January 13, 2011
Accepted: February 14, 2011
Published: March 02, 2011

In 2000, Lippard and co-workers reported an elegant example of fluorescein-based Zn^{2+} chemosensors (Zinpyr-1) containing the Zn^{2+} binding moiety, bis(2-pyridylmethyl)amine (DPA).[35] DPA can effectively quench the emission of fluorescein via photoinduced electron transfer (PET); upon addition of Zn^{2+} ions, strong fluorescence emission emerges owing to the formation of DPA/Zn^{2+} complex, which can efficiently block the PET process. Moreover, the cell permeability of Zinpyr-1 and intracellular imaging capability endows it with potent applications in neuroscience research. Recently, Xu et al. reported a novel Zn^{2+}-selective chemosensor, ZTRS, by combining the amide-containing DPA with fluorescent naphthalimide.[46] It shows excellent selectivity for Zn^{2+} ions over most competitive heavy and transition metal ions such as Fe^{2+}, Co^{2+}, Ni^{2+}, Cu^{2+}, Cd^{2+}, and Hg^{2+}. The ability to discriminate Zn^{2+} from Cd^{2+} ions and its in vivo imaging capability represent an important improvement in this field.

Apart from this, quinolines and their derivatives were the first fluorescent chemosensors used for the quantitative assay of Zn^{2+} ions.[1] In 1987, the first Zn^{2+} chemosensor, 6-methoxy-8-(*p*-toluenesulfonamido)quinoline (TSQ), was applied in the research of brain functions.[65] The excellent features of TSQ, such as pH-independent emission, nontoxicity, good selectivity, and prominent fluorescence enhancement, have rendered its broad applications in Zn^{2+}-related biological research.[1] Besides, numerous different quinoline derivatives-based Zn^{2+} chemosensors have also been developed in an effort to improve the detection performance.[31,59−64,66−72] According to the general criteria required for the imaging of Zn^{2+} ions at the cellular and subcellular level,[11,12] the rapid and reversible detection of Zn^{2+} ions is a prerequisite, in addition to other requirements such as high selectivity and biological compatibility (such as water solubility and nontoxicity). With this in mind, chemosensors with different binding affinities to Zn^{2+} ions are required to be used in varying circumstances considering the broad range of Zn^{2+} concentrations in different types of cells.[2,10] For instance, to monitor the dynamic variation of Zn^{2+} ions in firing neurons where Zn^{2+} concentrations are as high as ∼0.3 mM,[81] Zinpyr-1[35] with a subnanomolar dissociation constant might not be useful due to the saturated fluorescence signal. However, QZ2,[31] which possesses a dissociation constant at the micromolar level seems to be a suitable choice. Similarly, to image within cells where only trace amounts of Zn^{2+} ions are expected, Zinpyr-1[35] is a good candidate. Recently, Lippard and co-workers reported the synthesis of two 8-aminoquinoline-derivatized fluoresceins as rapid and reversible Zn^{2+} chemosensors, which exhibit ∼42 and ∼150-fold fluorescence enhancements upon addition of Zn^{2+} ions, respectively.[31] Because of the relatively low affinity to Zn^{2+} ions, they can reversibly respond to relatively high concentrations of Zn^{2+} ions, which is very important for the tracing of Zn^{2+} levels in certain tissues and organs (such as central nervous system and pancreatic tissues).

It is worthy of noting that the above examples of small molecule-based fluorometric Zn^{2+} sensors are typically subjected to limitations such as poor water solubility, less satisfactory detection sensitivity, and difficult to be integrated with other analyte-sensing capabilities. Moreover, considering their *in vivo* applications, small molecule fluorometric probes possess inherent limits such as rapid elimination and extravasation out of the vasculature, which greatly restricts the timing for measurements. On the other hand, stimuli-responsive polymers, which are capable of exhibiting reversible or irreversible changes in physical properties and/or chemical structures to variations in external environment, have recently been introduced into the design of novel sensing systems.[13,82−88]

Scheme 1. Schematic Illustration for the Fabrication of Thermoresponsive PEG-*b*-P(MEO$_2$MA-*co*-ZQMA) Double Hydrophilic Block Copolymer-Based Fluorescent Chemosensors of Zn^{2+} Ions and Temperature

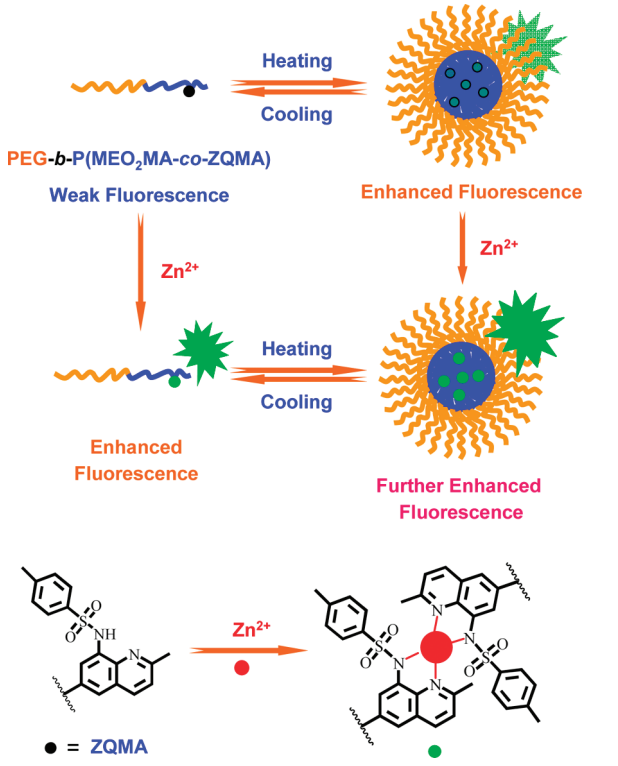

When analyte-recognizing receptor or analyte-reactive moieties and fluorophores are physically or chemically attached to the backbone or side chains of responsive polymers, these novel sensing systems can offer additional advantages such as improved water solubility, extended in vivo circulation times, larger accumulation capacity due to the enhanced permeability and retention (EPR) effect, and the facile integration of multifunctions such as sensing, imaging, and therapeutics.[13,88] In addition, the detection sensitivity and selectivity can be tuned via the reversible conformational changes, assembly/disassembly, and swelling/collapse of responsive polymer chains, polymeric assemblies, and microgels/nanogels, respectively.[82−87] We recently reported the synthesis of well-defined double hydrophilic block copolymers (DHBCs) bearing Hg^{2+}-reactive rhodamine B derivatives (RhBHA) in the thermoresponsive block, poly(ethylene glycol)-*b*-poly(*N*-isopropylacrylamide-*co*-RhBHA), PEG-*b*-P(NIPAM-*co*-RhBHA), which can serve as multifunctional sensors to pH, temperature, and Hg^{2+} ions.[85] Moreover, the detection sensitivity to Hg^{2+} and pH could be dramatically enhanced at elevated temperature due to thermo-induced formation of micelles possessing hydrophobic cores. In this case, Hg^{2+} and lowering solution pH can induce the chemical transformation of RhB moieties from the nonfluorescent spirolactam form to the highly fluorescent acyclic form. It would be highly desirable to explore whether thermoresponsive polymers covalently linked with small molecule sensing moieties functioning via the supramolecular recognition

Scheme 2. Synthetic Schemes Employed for the Preparation of Zn^{2+}-Recognizing Quinoline-Based Fluorescent Polymerizable Monomer, ZQMA (6)

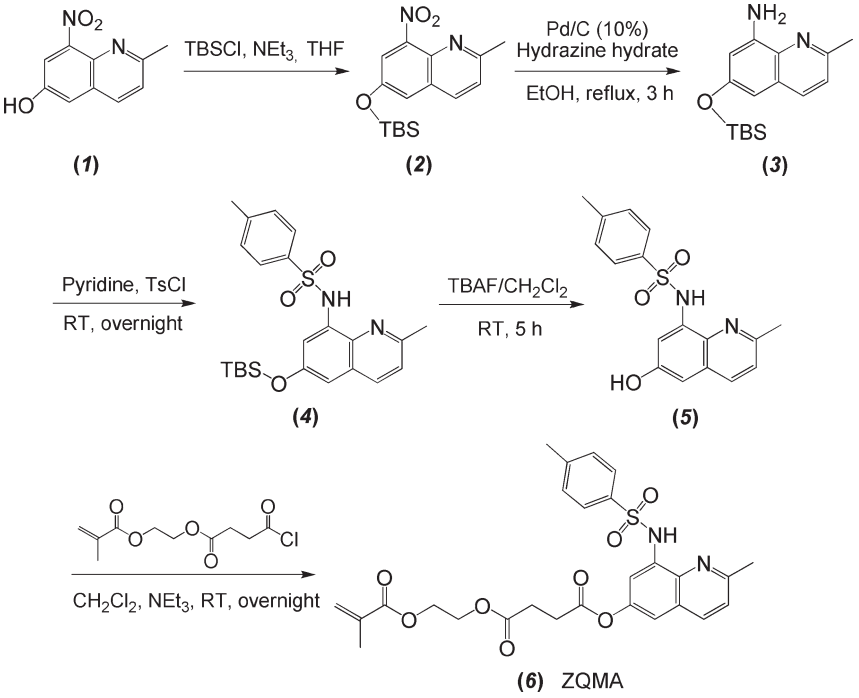

mechanism can still exhibit the above excellent features, aiming at the same time to develop novel responsive polymer-based metal ion probes. Besides, for PEG-*b*-P(NIPAM-*co*-RhBHA), the thermal sensing function can be only fixed in a specific range, i.e., across the thermal phase transition (~32 °C) of PNIPAM. Thus, it is quite advantageous to design sensing systems with tunable and more flexible thermal detection ranges.

In the current work, we fabricated a novel type of responsive double hydrophilic block copolymers (DHBCs)-based dual fluorescent chemosensors for temperature and Zn^{2+} ions possessing tunable detection sensitivity and reversible Zn^{2+} ion-binding capability (Scheme 1). A novel quinoline-based polarity-sensitive and Zn^{2+}-recognizing fluorescent monomer (ZQMA, **6**) was synthesized at first (Scheme 2). Well-defined DHBCs bearing quinoline-based Zn^{2+}-recognizing ZQMA moieties in the thermoresponsive block, PEG-*b*-P(MEO_2MA-*co*-OEGMA-*co*-ZQMA), were synthesized via the reversible addition- fragmentation chain transfer (RAFT) polymerization of 2-(2-methoxyethoxy)ethyl methacrylate (MEO_2MA), oligo(ethylene glycol) monomethyl ether methacrylate (OEGMA), and ZQMA, starting from the PEG-based macro-RAFT agent (Scheme 3). The OEGMA contents in the thermoresponsive block range from 0 to 12.0 mol % to tune the lower critical solution temperature (LCST). It was found that the fluorescence emission intensity of DHBCs can be considerably enhanced upon heating above the LCST. At temperatures below and above the critical micellization temperature (CMT), as-synthesized DHBCs in aqueous media exhibit prominent fluorescence enhancement upon addition of Zn^{2+} ions, with the detection limits down to ~3 nM and ~14 nM, respectively. Moreover, reversible binding between ZQMA moieties and Zn^{2+} ions at 37 °C can be achieved. This work represents the first example of purely aqueous-based polymeric Zn^{2+} sensors by integrating the well-developed small molecule Zn^{2+}-sensing moieties with stimuli-responsive DHBCs.

Scheme 3. Synthetic Schemes Employed for the Preparation of Well-Defined Thermoresponsive Double Hydrophilic Block Copolymers Covalently Labeled with ZQMA Moieties, PEG-*b*-P(MEO_2MA-*co*-OEGMA-*co*-ZQMA)

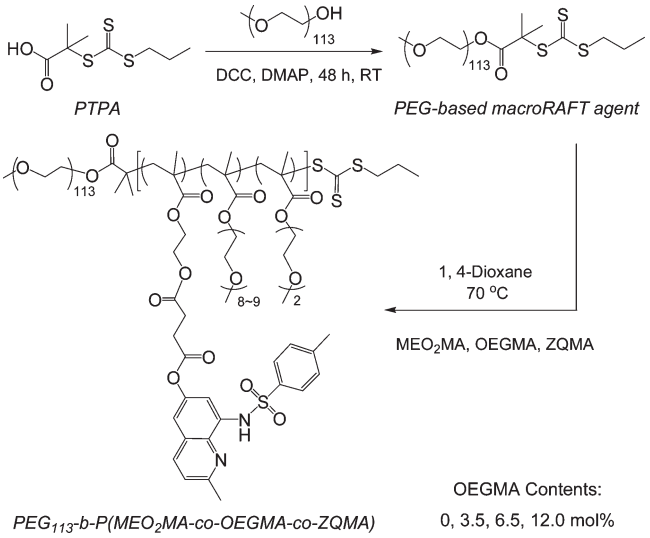

EXPERIMENTAL SECTION

Materials. Poly(ethylene glycol) monomethyl ether (PEG_{113}-OH, M_n = 5.0 kDa, M_w/M_n = 1.06, mean degree of polymerization, DP, is 113) was purchased from Aldrich and used as received. Oligo(ethylene glycol) monomethyl ether methacrylate (M_n = 475 g/mol, mean degree of polymerization, DP, is 8−9) purchased from Aldrich was passed through a neutral alumina column to remove the inhibitor and then stored at −20 °C prior

dx.doi.org/10.1021/ac200095f |*Anal. Chem.* 2011, 83, 2775–2785

to use. 2-(2-Methoxyethoxy)ethyl methacrylate (MEO_2MA, 95%, Aldrich) was dried over calcium hydride (CaH_2), distilled at reduced pressure, and then stored at −20 °C prior to use. 2,2′-Azoisobutyronitrile (AIBN) was recrystallized from 95% ethanol. Fetal bovine serum (FBS), penicillin, streptomycin, and Dulbecco's modified Eagle's medium (DMEM) were purchased from GIBCO and used as received. 4-Amino-3-nitrophenol (99%), *tert*-butylchlorodimethylsilane (TBSCl, 98%), Pd/C (10%), *p*-toluenesulfonyl chloride (TsCl, 99%), *N*,*N*′-dicyclohexylcarbodiimide (DCC), 4-dimethylaminopyridine (DMAP), hydrazine hydrate, tetrabutylammonium fluoride (TBAF), and all other reagents were purchased from Sinopharm Chemical Reagent Co. Ltd. and used as received. Tetrahydrofuran (THF) and toluene were dried by refluxing over sodium shavings and distilled just prior to use. Triethylamine (TEA), dichloromethane (CH_2Cl_2), and pyridine were dried over CaH_2 and distilled just prior to use. Nitrate salts (Ag^+, Al^{3+}, Ba^{2+}, Ca^{2+}, Co^{2+}, Cu^{2+}, Fe^{2+}, Fe^{3+}, Hg^{2+}, Li^+, Mg^{2+}, Mn^{2+}, Ni^{2+}, Pb^{2+}, Cd^{2+}, and Zn^{2+}) were used for all sensing experiments. Water was deionized with a Milli-Q SP reagent water system (Millipore) to a specific resistivity of 18.4 MΩ cm. 2-(3-Chlorocarbonylpropanoyloxy)-ethyl methacrylate,[89] 2-methyl-6-hydroxy-8-nitroquinoline,[90,91] 2-propylsulfanylthiocarbonyl sulfanyl-2-methyl propionic acid (PTPA),[92] and PEG-based macroRAFT agent[85] were synthesized according to literature procedures.

Sample Synthesis. Synthetic schemes employed for the preparation of quinoline-based polarity-sensitive and Zn^{2+}-recognizing fluorescent monomer (ZQMA, **6**) and ZQMA-labeled thermoresponsive DHBCs, PEG-*b*-P(MEO_2MA-*co*-OEGMA-*co*-ZQMA) are shown in Schemes 2 and 3.

*Synthesis of 2-Methyl-6-(tert-Butyldimethylsiloxy)-8-Aminoquinoline (**3**).* 2-Methyl-6-hydroxy-8-nitroquinoline (**1**, 3.0 g, 14.69 mmol) and TEA (3.19 mL, 22.07 mmol) were dissolved in anhydrous THF (40 mL) and cooled to 0 °C in an ice−water bath. TBSCl (2.66 g, 17.65 mmol) in anhydrous THF (10 mL) was added dropwise over 30 min. Then the reaction mixture was stirred at ambient temperature overnight. After filtration, the filtrate was evaporated to dryness on a rotary evaporator, and the crude product was purified by neutral alumina column chromatography using CH_2Cl_2 as the eluent. After drying in a vacuum oven overnight, **2** was obtained as a yellowish solid (4.21 g, yield: 90%).

Compound **2** (2.0 g, 6.28 mmol), Pd/C (10%) (0.40 g), and ethanol (40 mL) were mixed, heated to reflux, and degassed by bubbling with N_2 for 30 min. Hydrazine hydrate (0.61 mL, 12.50 mmol) was then added dropwise to the suspension for 10 min, and the reaction mixture was refluxed for 3 h. After filtration, the filtrate was evaporated to dryness on a rotary evaporator. The crude compound was further purified by basic alumina column chromatography using CH_2Cl_2 as the eluent. After drying in a vacuum oven overnight, **3** was obtained as an orange solid (1.05 g, yield: 58%). ^{1}H NMR ($CDCl_3$, δ, ppm, TMS; Figure S1a in the Supporting Information): 7.80, (1H, 4-Ar*H*-pyridyl), 7.18, (1H, 3-Ar*H*-pyridyl), 6.49−6.55 (2H, 5-Ar*H*-quinolyl and 7-Ar*H*-quinolyl), 4.97 (2H, -NH_2), 2.67 (3H, ArCH_3), 1.03 (9H, -Si$(CH_3)_2$C$(CH_3)_3$), and 0.25 (6H, -Si$(CH_3)_2$C$(CH_3)_3$).

*Synthesis of 2-Methyl-6-(tert-butyldimethylsiloxy)-8-(p-toluenesulfonamido)quinoline (**4**).* Compound **3** (0.85 g, 2.95 mmol) was dissolved in anhydrous pyridine (10 mL) and cooled to 0 °C in an ice−water bath. TsCl (0.67 g, 3.51 mmol) in anhydrous pyridine (5 mL) was then added dropwise over 30 min. The reaction mixture was stirred at 0 °C for 2 h and then overnight at room temperature. The mixture was subsequently poured into an ice−water mixture (100 mL) and left to stand at 4 °C for 2 h. The precipitated product was filtered off, washed with saturated $NaHCO_3$, and further purified by neutral alumina column chromatography using ethyl acetate as the eluent. After drying in a vacuum oven overnight, **4** was obtained as a white solid (0.75 g, yield: 57%). ^{1}H NMR ($CDCl_3$, δ, ppm, TMS; Figure S1b in the Supporting Information): 7.74−7.78 (3H, 4-Ar*H*-quinolyl, 2-Ar*H*-benzyl, and 6-Ar*H*-benzyl), 7.29 (1H, 3-Ar*H*-quinolyl), 7.10−7.19 (3H, 5-Ar*H*-quinolyl, 3-Ar*H*-benzyl, and 5-Ar*H*-benzyl), 6.68 (1H, 7-Ar*H*-quinolyl), 2.67 (3H, ArCH_3-quinolyl), 2.26 (3H, ArCH_3-benzyl), 1.03 (9H, -Si$(CH_3)_2$C$(CH_3)_3$), and 0.25 (6H, -Si$(CH_3)_2$C$(CH_3)_3$).

*Synthesis of Quinoline-Based Zn^{2+}-Recognizing Fluorescent Monomer (ZQMA, **6**).* Compound **4** (0.63 g, 1.42 mmol) and TBAF (0.44 g, 1.68 mmol) were dissolved in dry CH_2Cl_2 (25 mL) and stirred for 5 h at room temperature. Then the reaction solution was cooled to 0 °C in an ice−water bath, and TEA (0.31 mL, 2.14 mmol) was charged. The freshly prepared 2-(3-chlorocarbonylpropanoyloxy)ethyl methacrylate (0.42 g, 1.69 mmol) in dry CH_2Cl_2 (15 mL) was then added dropwise over 30 min. The reaction mixture was stirred at room temperature overnight followed by washing with saturated $NaHCO_3$ (3 × 40 mL) and saturated NaCl solution. The organic layer was collected and dried over anhydrous Na_2SO_4. After filtration, the filtrate was evaporated to dryness on a rotary evaporator and the residues were further purified by neutral alumina column chromatography using ethyl acetate/CH_2Cl_2 (5:95 v/v) as the eluent. After drying in a vacuum oven overnight, **6** was obtained as an orange solid (0.10 g, yield: 13%). ^{1}H NMR ($CDCl_3$, δ, ppm, TMS, Figure S1c in the Supporting Information): 7.86 (1H, 4-Ar*H*-quinolyl), 7.77 (2H, 2-Ar*H*-benzyl, and 6-Ar*H*-benzyl), 7.55 (1H, 7-Ar*H*-quinolyl), 7.23 (1H, 3-Ar*H*-quinolyl), 7.09−7.16 (3H, 5-Ar*H*-quinolyl, 3-Ar*H*-benzyl, and 5-Ar*H*-benzyl), 6.08 and 5.52 (2H, CH_2=C(CH_3)-), 5.26 (1H, -N*H*-), 4.35 (4H, -OCH_2CH_2O-), 2.76−2.90 (4H, -OCOCH_2CH_2OCO-), 2.67 (3H, ArCH_3-quinolyl), 2.26 (3H, ArCH_3-benzyl)), and 1.89 (3H, CH_2=C(CH_3)-).

Synthesis of PEG-Based MacroRAFT Agent (Scheme 3). PEG-based macroRAFT agent was prepared according to similar procedures reported previously.[85] In a typical procedure, PEG_{113}−OH (10.0 g, 2.0 mmol) was dissolved in anhydrous toluene (25 mL) and then azeotropic distillation was carried out under reduced pressure at 50 °C to remove most of the solvents. PTPA (0.57 g, 2.39 mmol) and dry CH_2Cl_2 (100 mL) were then added. After cooling to 0 °C in an ice−water bath, a mixture containing DCC (0.83 g, 4.0 mmol), DMAP (49 mg, 0.4 mmol), and dry CH_2Cl_2 (20 mL) was added dropwise over 1 h. The reaction mixture was then stirred at room temperature for 48 h. After removal of insoluble salts by filtration, the filtrates were concentrated on a rotary evaporator and then precipitated into an excess of cold diethyl ether. The above dissolution−precipitation cycle was repeated three times. After drying in a vacuum oven overnight, PEG_{113} macroRAFT agent was obtained as a slightly yellowish powder (8.4 g, yield, 80%; $M_{n,GPC}$ = 5.0 kDa; M_w/M_n = 1.07).

Synthesis of PEG-b-P(MEO_2MA-co-OEGMA-co-ZQMA) DHBCs (Scheme 3). PEG-*b*-P(MEO_2MA-*co*-OEGMA-*co*-ZQMA) with OEGMA contents in the ZQMA-labeled thermoresponsive block ranging from 0 to 12.0 mol % were synthesized via RAFT polymerization. Typically, PEG-based macroRAFT agent (0.21 g, 0.04 mmol), MEO_2MA (0.753 g, 4.0 mmol), ZQMA (22 mg, 0.04 mmol), AIBN (2 mg, 0.012 mmol), and 1,4-dioxane (5 mL) were charged into a glass ampule equipped with a magnetic stirring bar.

The glass ampule was carefully degassed via three freeze−pump−thaw cycles and then sealed under vacuum. After thermostatting at 70 °C in an oil bath and stirring overnight, the reaction tube was quenched into liquid nitrogen, opened, and diluted with 1,4-dioxane. The mixture was then precipitated into an excess of diethyl ether. The above dissolution−precipitation cycle was repeated three times to afford PEG-*b*-P(MEO_2MA-*co*-ZQMA) (0.54 g, 56%). The molecular weight and molecular weight distribution of PEG-*b*-P(MEO_2MA-*co*-ZQMA) were determined by GPC using THF as the eluent, revealing an M_n of 18.0 kDa and an M_w/M_n of 1.29 (Figure S2 in the Supporting Information). The degree of polymerization, DP, of PEG-*b*-P(MEO_2MA- *co*-ZQMA) was determined to be 70 by ^{1}H NMR analysis in $CDCl_3$. Thus, the polymer was denoted as PEG_{113}-*b*-P(MEO_2MA-*co*-ZQMA)$_{70}$. ZQMA content in P(MEO_2MA-*co*-ZQMA) block was determined to be 0.66 mol % by UV−vis spectroscopy in ethanol by using ZQMA monomer as the calibration standard. With similar procedures followed, three PEG-*b*-P(MEO_2MA-*co*-OEGMA-*co*-ZQMA) DHBCs were also prepared by varying the monomer feed contents (Figure S2 in the Supporting Information): PEG_{113}-*b*-P($MEO_2MA_{0.965}$-*co*-OEG-$MA_{0.035}$-*co*-ZQMA)$_{72}$ (M_n = 19.3 kDa, M_w/M_n = 1.28; ZQMA content: 0.64 mol %), PEG_{113}-*b*- P($MEO_2MA_{0.935}$-*co*-OEG-$MA_{0.065}$-*co*-ZQMA)$_{65}$ (M_n = 18.2 kDa, M_w/M_n = 1.35; ZQMA content, 0.61 mol %), and PEG_{113}-*b*-P($MEO_2MA_{0.88}$-*co*-OEG-$MA_{0.12}$-*co*-ZQMA)$_{60}$ (M_n = 18.0 kDa, M_w/M_n = 1.39; ZQMA content, 0.59 mol %).

Cell Culture and in Vitro Fluorescence Imaging of Zn^{2+} Ions. HeLa cells were cultured in Dulbecco's modified Eagle medium (DMEM) supplemented with 10% fetal bovine serum (FBS), penicillin (100 units/mL), and streptomycin (100 μg/mL) at 37 °C in a CO_2/air (5:95) incubator for 2 days. For fluorescence imaging, cells were transferred to DMEM containing 1% FBS and 2.0 g/L PEG_{113}-*b*-P(MEO_2MA-*co*-ZQMA)$_{70}$ ([ZQMA] = 5.0×10^{-5} M) at 37 °C in a CO_2/air (5:95) incubator for 4 h. The cells were washed twice with PBS buffer prior to the addition of Zn^{2+} ions. Zn^{2+} ions were then introduced to the cultured cells to target a final concentration of 200 μM, and the mixture was further incubated for 30 min.

Characterization. All ^{1}H nuclear magnetic resonance (NMR) spectra were recorded on a Bruker AV300 NMR spectrometer (resonance frequency of 300 MHz for ^{1}H NMR) operated in the Fourier transform mode. $CDCl_3$ was used as the solvent. Molecular weights and molecular weight distributions were determined by gel permeation chromatography (GPC) equipped with a Waters 1515 pump and a Waters 2414 differential refractive index detector (set at 30 °C). It used a series of two linear Styragel columns (HR2 and HR4) at an oven temperature of 45 °C. The eluent was THF at a flow rate of 1.0 mL/min. A series of low polydispersity polystyrene standards were employed for calibration. All UV−vis spectra were acquired on a Unico UV/vis 2802PCS spectrophotometer. The transmittance of the aqueous solutions was acquired at a wavelength of 700 nm. A thermostatically controlled cuvette was employed, and the heating rate was 0.2 °C min^{-1}. Dynamic laser light scattering (LLS) measurements were conducted on a commercial spectrometer (ALV/DLS/SLS-5022F) equipped with a multitau digital time correlator (ALV5000) and a cylindrical 22 mW UNIPHASE He−Ne laser (λ_0 = 632 nm) as the light source. Scattered light was collected at a fixed angle of 90° for a duration of ~5 min. Distribution averages and particle size distributions were computed using cumulants analysis and CONTIN routines. All data were averaged over three measurements. Fluorescence spectra were recorded using a RF-5301/PC (Shimadzu) spectrofluorometer. The temperature of the water-jacketed cell holder was controlled by a programmable circulation bath. The slit widths were set at 5 nm for both excitation and emission. The fluorescence images of HeLa cells were acquired using Nikon Eclipse TE2000-U inverted microscopy at room temperature.

RESULTS AND DISCUSSION

Synthesis and Thermo-Induced Micellization of ZQMA-Labeled DHBCs. Well-defined DHBCs bearing Zn^{2+}-sensing moieties in the thermoresponsive block, PEG-*b*-P(MEO_2MA-*co*-ZQMA) and PEG-*b*-P(MEO_2MA-*co*-OEGMA-*co*-ZQMA), were synthesized via reversible addition−fragmentation chain transfer (RAFT) polymerization by using PEG-based macroRAFT agent (Schemes 2 and 3). Novel polymerizable Zn^{2+}-recognizing fluorescent monomer, ZQMA, was prepared at first. The reaction of 2-methyl-6-hydroxy-8-nitroquinoline (**1**) with TBSCl leads to TBS-protected **2** with a yield of ~90%. This was followed by the reduction of nitro functionality to amine with an excess of hydrazine hydrate in the presence of Pd/C, affording 2-methyl-6-(*tert*-butyldimethylsiloxy)-8-aminoquinoline (**3**). Its chemical structure was confirmed by ^{1}H NMR analysis as shown in Figure S1a in the Supporting Information. The obtained compound **3** was reacted with TsCl in dry pyridine to afford 2-methyl-6-(*tert*-butyldimethylsiloxy)-8-(*p*-toluenesulfonamido)-quinoline (**4**). ^{1}H NMR spectrum of **4** is shown in Figure S1b in the Supporting Information, together with the peak assignments. We can clearly observe the appearance of a new resonance signal at 2.26 ppm, which can be ascribed to methyl protons adjacent to the benzene ring (peak *l*). Moreover, integral ratios between characteristic peaks confirmed the quantitative functionalization.

In the final step, **4** was deprotected with TBAF at first to give hydroxyl-containing 2-methyl-6-hydroxy-8-(*p*-toluenesulfonamido)quinoline (**5**), which was immediately, without purification, reacted with freshly prepared 2-(3-chlorocarbonylpropanoyloxy)ethyl methacrylate to afford the target product, quinoline-based Zn^{2+}-recognizing fluorescent monomer (ZQMA, **6**). The chemical structure of ZQMA was confirmed by ^{1}H NMR analysis (Figure S1c in the Supporting Information). Relative integral ratios between characteristic resonance signals (peaks a, e, f, h, m, and o) are determined to be 3:2:2:3:2:3, accompanied with the presence of methacrylate double bond signals at 5.52 and 6.08 ppm. This indicates the successful preparation of Zn^{2+}-sensing monomer **6**.

Well-defined DHBCs bearing quinoline-based Zn^{2+}-sensitive moieties in the thermoresponsive block were synthesized via RAFT polymerization of MEO_2MA and ZQMA in the presence of PEG-based macroRAFT agent in 1,4-dioxane at 70 °C with an M_n of 18.0 kDa and an M_w/M_n of 1.29 based on GPC analysis. The content of ZQMA moieties in the P(MEO_2MA-*co*-ZQMA) block was determined to be ~0.66 mol % by UV−vis spectroscopy. With similar procedures followed, another three PEG-*b*-P(MEO_2MA-*co*-OEGMA-*co*-ZQMA) samples with the OEGMA molar contents being 3.5, 6.5, and 12.0 mol % were also synthesized.

Possessing two ethylene oxide repeating units in the monomer, $PMEO_2MA$ homopolymer possesses a lower critical solution temperature (LCST) phase transition at ~26 °C, just like those exhibited by PNIPAM in aqueous solutions (LCST ~ 32 °C).[93] $PMEO_2MA$ molecularly dissolves in cold and dilute aqueous solution but is insoluble above the LCST. It has been

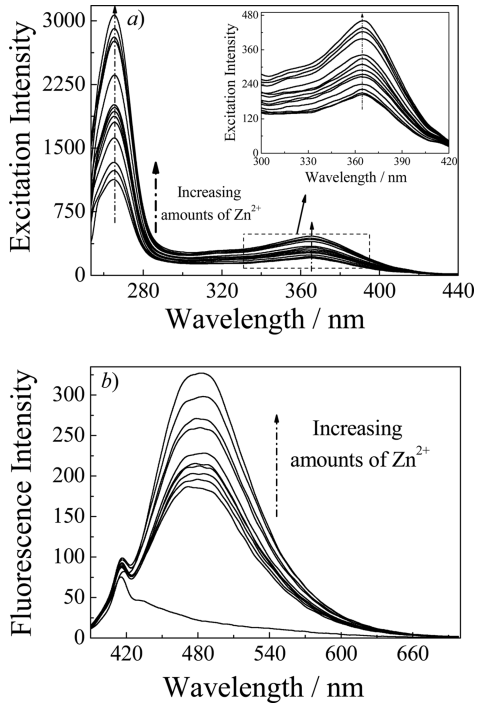

Figure 1. Fluorescence (a) excitation (λ_{em} = 482 nm) and (b) emission (λ_{ex} = 364 nm) spectra (slit widths, excitation 5 nm, emission 5 nm; 20 °C) recorded for the aqueous solution (pH 7.4, phosphate buffer) of PEG_{113}-*b*-P(MEO_2MA-*co*-ZQMA)$_{70}$ (0.2 g/L, [ZQMA] = 5.0×10^{-6} M; 20 °C) upon gradual addition of (a) 0.2−1.0 equiv and (b) 0.4−4.0 equiv (relative to ZQMA moieties) of Zn^{2+} ions. The inset in Figure 1a shows the enlarged excitation spectra in the wavelength range of 300−420 nm.

well-established that the copolymerization of highly hydrophilic OGEMA with MEO_2MA can lead to the facile tuning of LCST in the range of 26−90 °C for the copolymer.[94] Thermo-induced micellization of PEG-*b*-P(MEO_2MA-*co*-ZQMA) and PEG-*b*-P(MEO_2MA-*co*-OEGMA-*co*-ZQMA) DHBCs was then investigated by temperature-dependent optical transmittance and dynamic laser light scattering (LLS). Temperature-dependent transmittance measurements demonstrated that PEG_{113}-*b*-P(MEO_2MA-*co*-ZQMA)$_{70}$ DHBCs undergo thermo-induced micellization above ~25 °C, due to the LCST phase behavior of MEO_2MA-containing blocks (Figure S3 in the Supporting Information). Similarly, PEG-*b*-P(MEO_2MA-*co*-OEGMA-*co*-ZQMA) DHBCs with the OEGMA molar contents being 3.5, 6.5, and 12.0 mol % possess critical micellization temperatures (CMTs) of ~30 °C, 32 °C, and 39 °C respectively (Figure S3 in the Supporting Information). The tuning of thermal phase transition temperatures with varying OEGMA molar contents has been well-documented by previous literature reports.[93] As revealed by dynamic LLS results, PEG_{113}-*b*-P(MEO_2MA-*co*-ZQMA)$_{70}$ that originally dissolves as unimers at 20 °C self-assembles at 37 °C into P(MEO_2MA-*co*-ZQMA)-core aggregates with an intensity-average hydrodynamic radius, $\langle R_h \rangle$, of 23 nm and size polydispersity of 0.128 (Figure S4 in the Supporting Information).

PEG-*b*-P(MEO_2MA-*co*-ZQMA) Unimers as Sensitive and Selective Fluorescent Chemosensors for Zn^{2+} Ions. We then at first investigated the Zn^{2+}-sensing capability of PEG-*b*-P(MEO_2MA-*co*-ZQMA) in their unimer state at 20 °C. It has been well-documented that the fluorescence emission of quinoline-based small molecule Zn^{2+} probes can be effectively quenched in the absence of Zn^{2+} ions; upon addition of Zn^{2+} ions, considerable fluorescence enhancement can be achieved.[59−63,65,67−72] In the current work, we designed a novel polymerizable quinoline-based monomer with the 2-position substituted with a methyl group and the 8-position modified with a toluenesulfonamido moiety. For small fluorometric probes containing a similar structural motif, they can selectively and effectively recognize Zn^{2+} ions and exhibit prominent fluorescence enhancement (Schemes 1 and 2). In an effort to solve the issue of poor water-solubility, we copolymerized ZQMA into the thermoresponsive block and synthesized PEG-*b*-P(MEO_2MA-*co*-ZQMA) and PEG-*b*-P(MEO_2MA-*co*-OEGMA-*co*-ZQMA).

Typical fluorescence excitation and emission spectra obtained for the aqueous solution (pH 7.4 phosphate buffer) of PEG_{113}-*b*-P(MEO_2MA-*co*-ZQMA)$_{70}$ (0.2 g/L, [ZQMA] = 5.0×10^{-6} M) upon gradual addition of Zn^{2+} ions are shown in Figure 1. The excitation spectra of PEG_{113}-*b*-P(MEO_2MA-*co*-ZQMA)$_{70}$ exhibit a main peak at ~265 nm and a broad band at ~364 nm. Upon gradual addition of 0−1.0 equiv of Zn^{2+} ions (relative to that of ZQMA residues), we can observe the dramatic enhancement of these two bands with a negligible peak shift, indicating a perturbation of the quinoline conjugated system presumably due to the coordination of Zn^{2+} ions with nitrogen atoms within quinoline and the sulfonamido moiety.[69] When excited at 364 nm, the aqueous solution of PEG_{113}-*b*-P(MEO_2MA-*co*-ZQMA)$_{70}$ (0.2 g/L) exhibit almost undetectable fluorescence emissions in the absence of Zn^{2+} ions. Similar phenomenon has been reported for small molecule quinoline-based probes bearing comparable chemical structures.[59,65,69] This indicates that the incorporation of ZQMA moiety into DHBCs does not alter the photophysical properties. Moreover, the fluorescence emission intensity at 482 nm substantially increases (~9.4-fold) upon addition of 0.5 equiv of Zn^{2+} ions and gradually stabilizes out in the presence of >4.0 equiv of Zn^{2+} ions. An ~15-fold cumulative fluorescence enhancement can be observed in the Zn^{2+} concentration range of 0−4.0 equiv (Figures 1b and 2). At a polymer concentration of 1.0 g/L, the enhancement of fluorescence emission in the presence of 4.0 equiv of Zn^{2+} ions can be clearly discerned by the naked eye (Figure 3c); thus, ZQMA-labeled DHBCs in aqueous media at room temperature can serve as a "visible" fluorometric probe for Zn^{2+} ions. If we arbitrarily define the detection limit as the Zn^{2+} concentration at which a 10% fluorescence enhancement relative to the blank sample can be measured by employing 0.2 g/L aqueous solution of PEG_{113}-*b*-P(MEO_2MA-*co*-ZQMA)$_{70}$, the Zn^{2+} detection limit was determined to be 3.0 nM, which is quite comparable to or considerably lower than the Zn^{2+} concentration within many types of cells.[2,10,85] The relatively high sensitivity accompanied with the excellent water solubility of PEG_{113}-*b*-P(MEO_2MA-*co*-ZQMA)$_{70}$-based Zn^{2+} probes augurs well for the promising prospect in terms of their potential applications.

The detection selectivity of PEG_{113}-*b*-P(MEO_2MA-*co*-ZQMA)$_{70}$ toward Zn^{2+} ions over other common metal ions was then investigated (Figure 4). It was found that among a series of biorelevant metal ions and common transition metal ions including Ag^+, Al^{3+}, Ba^{2+}, Ca^{2+}, Co^{2+}, Cu^{2+}, Fe^{2+}, Fe^{3+}, Hg^{2+}, Li^+, Mg^{2+}, Mn^{2+}, Ni^{2+}, Pb^{2+}, Cd^{2+}, and Zn^{2+} (4.0 equiv), only Zn^{2+} ions exhibits the most prominent fluorescence enhancement (~15-fold). The presence of 4.0 equiv Cd^{2+} ions induces ~8.7-fold emission enhancement. Important biorelated metal ions such as Na^+, K^+, Ca^{2+}, and Mg^{2+}, which often exist at high concentrations in most living cells, resulted in negligible fluorescence enhancement, as compared with

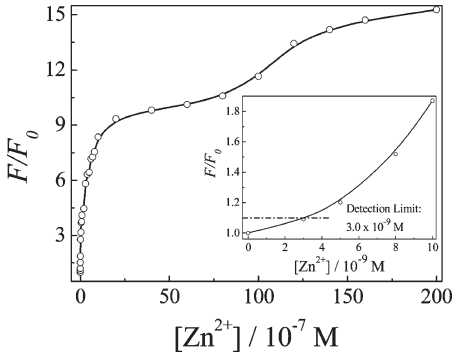

Figure 2. Relative fluorescence intensity changes, F/F_0, (λ_{ex} = 364 nm, λ_{em} = 482 nm; slit widths, excitation 5 nm, emission 5 nm; 20 °C) recorded for the aqueous solution (pH 7.4 phosphate buffer) of PEG_{113}-*b*-$P(MEO_2MA$-*co*-$ZQMA)_{70}$ (0.2 g/L, [ZQMA] = 5.0×10^{-6} M) upon gradual addition of 0−4.0 equiv (relative to ZQMA moieties) of Zn^{2+} ions. F and F_0 represent the fluorescence intensity in the presence and absence of Zn^{2+} ions, respectively. The inset shows the determination of the Zn^{2+} detection limit.

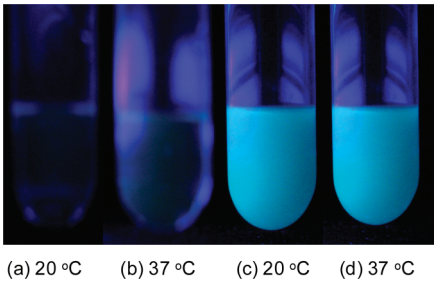

Figure 3. Photographs recorded under 365 nm UV lamp for aqueous solutions (pH 7.4 phosphate buffer) of PEG_{113}-*b*-$P(MEO_2MA$-*co*-$ZQMA)_{70}$ (1.0 g/L, [ZQMA] = 2.5×10^{-5} M) before (a, b) and after (c, d) addition of 4.0 equiv of Zn^{2+} ions.

that of Zn^{2+} ions. This can be ascribed to the poor coordination capability of these abundant cations with ZQMA moieties. These results also agree quite well with those reported for Zn^{2+} probes based on small molecule quinoline derivatives.[59,65,69,90,91] In addition, fluorescence spectra recorded in the presence of Zn^{2+} ions (4.0 equiv) and 4.0 equiv of competing metal ions (Al^{3+}, Ba^{2+}, Ca^{2+}, Co^{2+}, Cu^{2+}, Fe^{2+}, Fe^{3+}, Ag^{+}, Hg^{2+}, Li^{+}, Mg^{2+}, Mn^{2+}, Ni^{2+}, Pb^{2+}, and Cd^{2+}) further revealed that other metal ions, except for Cu^{2+}, Hg^{2+}, and Cd^{2+} ions, do not interfere with Zn^{2+}-induced fluorescence enhancements (Figure 5). The well-known fluorescence quencher, Cu^{2+} ions (originating from its unique atomic structure), can bind more strongly with nitrogen atoms of the quinoline structure than Zn^{2+} ions, thus it can seriously interfere with the fluorescence enhancement of ZQMA moieties by Zn^{2+} ions.[91] The interference of Cd^{2+} ions with Zn^{2+} sensing typically exists in many previously reported Zn^{2+}-sensing systems,[62,66,68,70] which remains to be a less well-solved issue toward the development of perfect Zn^{2+} probes.[12,95] Interestingly, concentrations of Cu^{2+}, Hg^{2+}, and Cd^{2+} ions in living cells are quite low, especially for Hg^{2+} ions. Thus, the presence of trace amount of Cu^{2+}, Hg^{2+}, and Cd^{2+} ions does not exclude the application of PEG_{113}-*b*-$P(MEO_2MA$-*co*-$ZQMA)_{70}$ for Zn^{2+} imaging and sensing in living cells. On the basis of the above results, we conclude that PEG_{113}-*b*-$P(MEO_2MA$-*co*-$ZQMA)_{70}$ DHBCs in the unimer state can serve as highly selective and sensitive fluorescent chemosensors for Zn^{2+} ions.

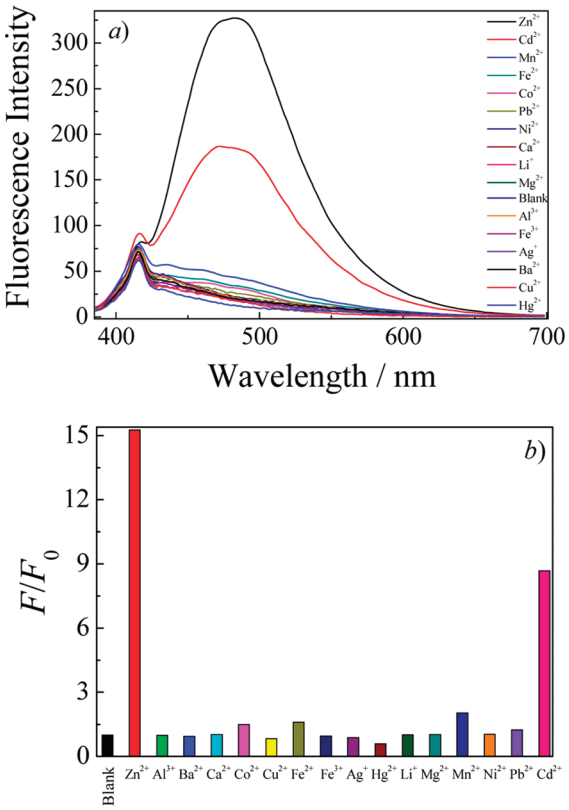

Figure 4. (a) Fluorescence emission spectra and (b) relative fluorescence intensity (λ_{ex} = 364 nm, λ_{em} = 482 nm; slit widths, excitation 5 nm, emission 5 nm; 20 °C) recorded for the aqueous solution (pH 7.4 phosphate buffer) of PEG_{113}-*b*-$P(MEO_2MA$-*co*-$ZQMA)_{70}$ (0.2 g/L, [ZQMA] = 5.0×10^{-6} M) upon addition of 4.0 equiv (relative to ZQMA moieties) of various metal ions (Zn^{2+}, Al^{3+}, Ba^{2+}, Ca^{2+}, Co^{2+}, Cu^{2+}, Fe^{2+}, Fe^{3+}, Ag^{+}, Hg^{2+}, Li^{+}, Mg^{2+}, Mn^{2+}, Ni^{2+}, Pb^{2+}, and Cd^{2+}), respectively.

PEG-*b*-P(MEO$_2$MA-*co*-OEGMA-*co*-ZQMA) Micelles as Dual Fluorescent Chemosensors for Zn^{2+} Ions and Temperatures. It has been well-documented that the quantum yields of many fluorescent organic dyes can be typically enhanced in the hydrophobic microenvironment compared to those in a more hydrophilic microenvironment.[83−85] As PEG_{113}-*b*-$P(MEO_2MA$-*co*-$ZQMA)_{70}$ self-assembles into micelles above the CMT (Figures S3 and S4 in the Supporting Information), accompanied with the formation of hydrophobic $P(MEO_2MA$-*co*-$ZQMA)_{70}$ cores, we expect that PEG_{113}-*b*-$P(MEO_2MA$-*co*-$ZQMA)_{70}$ can also act as a novel fluorescent thermometer. In the absence of Zn^{2+} ions, fluorescence emission intensity of the aqueous solution of PEG_{113}-*b*-$P(MEO_2MA$-*co*-$ZQMA)_{70}$ at 482 nm exhibits negligible changes at temperatures below 25 °C, and further heating to the temperature range of 26−34 °C leads to the abrupt increase of emission intensity (~6.0-fold enhancement), which well correlates with the thermo-induced micellization process (Figures 3b and 6; Figures S3−S5 in the Supporting Information).

Considering that the LCST of thermoresponsive $P(MEO_2MA$-*co*-OEGMA) can be facilely tuned by varying the OEGMA molar contents,[94] we further investigated the thermo-induced emission enhancement of PEG-*b*-$P(MEO_2MA$-*co*-OEGMA-*co*-ZQMA) DHBCs with varying OEGMA contents. As shown in Figure S5 in the Supporting Information, fluorescence emission intensity

dx.doi.org/10.1021/ac200095f |*Anal. Chem.* 2011, 83, 2775–2785

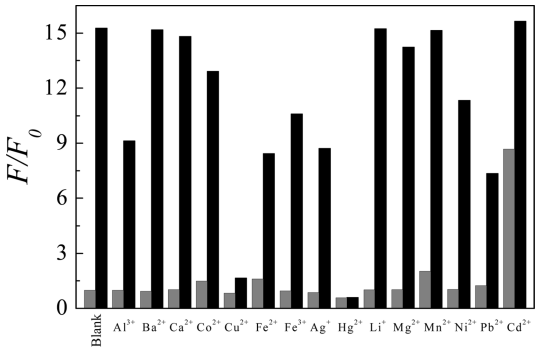

Figure 5. Selectivity of double hydrophilic block copolymer, PEG_{113}-*b*-P(MEO_2MA-*co*-ZQMA)$_{70}$, chemosensors (0.2 g/L, [ZQMA] = 5.0×10^{-6} M) for Zn^{2+} ions in the presence of other metal ions. The fluorescence response (λ_{ex} = 364 nm, λ_{em} = 482 nm; slit widths, excitation 5 nm, emission 5 nm; 20 °C) was normalized with respect to the initial fluorescence intensity of the blank sample. F and F_0 represent the fluorescence intensity of chemosensors in the presence and absence of metal ions, respectively. Gray bars: F/F_0 ratios upon addition of 4.0 equiv of different metal ions: Al^{3+}, Ba^{2+}, Ca^{2+}, Co^{2+}, Cu^{2+}, Fe^{2+}, Fe^{3+}, Hg^{2+}, Li^{+}, Mg^{2+}, Mn^{2+}, Ni^{2+}, Pb^{2+}, and Cd^{2+}, respectively. Black bars: F/F_0 ratios upon addition of 4.0 equiv of different metal ions followed by the addition of 4.0 equiv of Zn^{2+}, respectively.

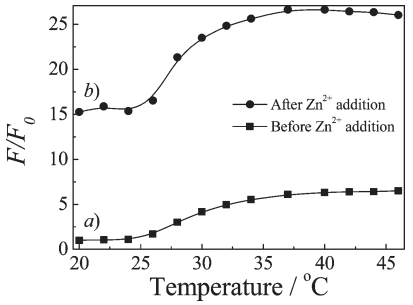

Figure 6. Changes in relative fluorescence intensities (λ_{ex} = 364 nm, λ_{em} = 482 nm; slit widths, excitation 5 nm, emission 5 nm) recorded in the temperature range of 20−46 °C for the aqueous solution (pH 7.4 phosphate buffer) of PEG_{113}-*b*-P(MEO_2MA-*co*-ZQMA)$_{70}$ (0.2 g/L, [ZQMA] = 5.0×10^{-6} M) (a) before and (b) after the addition of 4.0 equiv of Zn^{2+} ions (relative to ZQMA moieties).

of PEG-*b*-P(MEO_2MA-*co*-OEGMA-*co*-ZQMA) with OEGMA molar contents being 3.5, 6.5, to 12.0 mol % exhibit ~10.4-fold, 3.6-fold, and 7.1-fold emission enhancement, respectively, upon heating. The effective detection ranges vary from 30 to 34 °C, 32−36 °C, and 39−42 °C for these three PEG-*b*-P(MEO_2MA-*co*-OEGMA-*co*-ZQMA) samples. These optimum fluorometric thermal detection ranges again agree quite well with the thermal phase transitions (Figure S3 in the Supporting Information). Thus, the thermal detection ranges of ZQMA-labeled PEG-*b*-P(MEO_2MA-*co*-OEGMA-*co*-ZQMA) can be varied in the range of 26−42 °C by tuning the OEGMA contents.

In the presence of 4.0 equiv of Zn^{2+} ions (relative to ZQMA moieties), it was found that the fluorescence emission of the PEG_{113}-*b*-P(MEO_2MA-*co*-ZQMA)$_{70}$ also exhibits thermo-induced enhancement due to the thermoresponsive nature of the P(MEO_2MA-*co*-ZQMA) block. As shown in Figure 6b, the fluorescence intensity at 482 nm increased ~1.7-fold upon heating from 20 to 37 °C. As the fluorescence intensity of

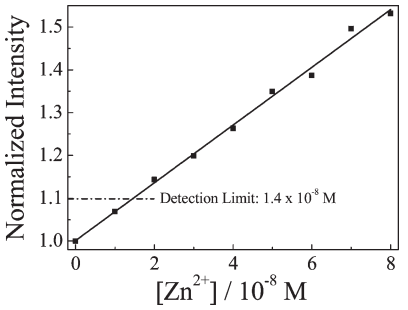

Figure 7. Changes in relative fluorescence intensities (λ_{ex} = 364 nm, λ_{em} = 482 nm; slit widths, exciatation 5 nm, emission 5 nm) at 37 °C recorded for the aqueous solution (pH 7.4 phosphate buffer) of PEG_{113}-*b*-P(MEO_2MA-*co*-ZQMA)$_{70}$ (0.2 g/L, [ZQMA] = 5.0×10^{-6} M) upon gradual addition of Zn^{2+} ions.

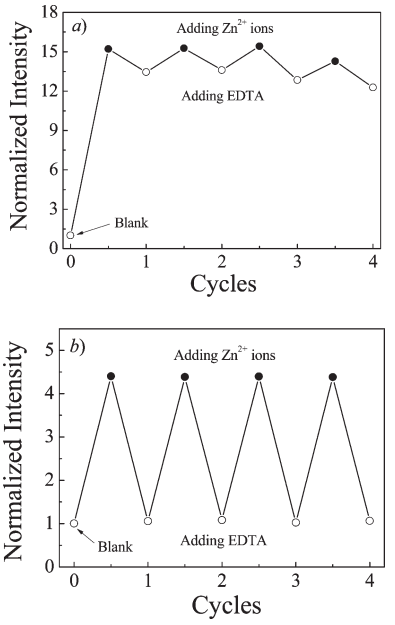

Figure 8. Changes in relative fluorescence intensities (λ_{ex} = 364 nm, λ_{em} = 482 nm; slit widths, excitation 5 nm, emission 5 nm) recorded for the aqueous solution (pH 7.4 phosphate buffer) of PEG_{113}-*b*-P(MEO_2MA-*co*-ZQMA)$_{70}$ (0.2 g/L, [ZQMA] = 5.0×10^{-6} M) upon sequential addition of 4.0 equiv of Zn^{2+} ions and EDTA at (a) 20 °C and (b) 37 °C, respectively. Four cycles were tested in each case.

PEG_{113}-*b*-P(MEO_2MA-*co*-ZQMA)$_{70}$ in aqueous solution in the absence of Zn^{2+} also exhibits an enhancement (~6.0-fold) at 37 °C relative to that at 20 °C, the Zn^{2+} detection limit might vary based on the current definition of the detection limit, i.e., 10% emission enhancement relative to the blank sample. As shown in Figure 7, the detection limit to Zn^{2+} ions changes from ~3.0 nM at 20 °C to ~14.0 nM at 37 °C. This can be ascribed to enhanced background emission. Considering that Zn^{2+} ions within living cells can vary from the nanomolar level to ~0.3 mM,[2,10] the observed thermo-modulated detection limits for PEG_{113}-*b*-P(MEO_2MA-*co*-ZQMA)$_{70}$ in aqueous media at varying temperatures might provide to be an additional advantage under certain circumstances.

Interestingly, compared with that of PEG_{113}-*b*-P(MEO_2MA-*co*-ZQMA)$_{70}$ at 20 °C, this DHBC-based Zn^{2+} chemosensor exhibits reversible on/off switchable fluorescence emissions at

Figure 9. Fluorescent images (330/385 nm excitation filter in combination with long pass 420 nm barrier filter) of (a) HeLa cells incubated with 2.0 g/L PEG_{113}-*b*-P(MEO_2MA-*co*-ZQMA)$_{70}$ (50.0 μM ZQMA residues) at 37 °C for 4 h, (b) HeLa cells incubated with 2.0 g/L PEG_{113}-*b*-P(MEO_2MA-*co*-ZQMA)$_{70}$ (50.0 μM ZQMA residues) at 37 °C for 4 h and followed by addition of 200 μM Zn^{2+} ions, and (c) a bright field image of the cells in panel b.

37 °C upon sequential addition of Zn^{2+} ions and EDTA, which can effectively recognize and capture Zn^{2+} ions. As shown in Figure 8, the fluorescence emission of PEG_{113}-*b*-P(MEO_2MA-*co*-ZQMA)$_{70}$ in the presence of 4.0 equiv of Zn^{2+} ions at 20 °C cannot be restored to the original nonfluorescent state upon EDTA addition (Figure 8a), though the fluorescence intensity can be modulated to some extent. However, when heated to 37 °C, the fluorescence emission of PEG_{113}-*b*-P(MEO_2MA-*co*-ZQMA)$_{70}$ can be dramatically enhanced in the presence of Zn^{2+} ions (4.4-fold); upon addition of EDTA, it almost completely restores to the original value obtained in the absence of Zn^{2+} ions (Figure 8b). Moreover, the on/off switchable fluorescence emission of PEG_{113}-*b*-P(MEO_2MA-*co*-ZQMA)$_{70}$ in aqueous media upon sequential addition of Zn^{2+} ions and EDTA can be cycled for several times. This is a very important result due to that in many areas of Zn^{2+}-related biological research, high Zn^{2+}-affinity chemosensors are not always required considering that Zn^{2+} concentrations in different cells can vary dramatically, i.e., ranging from nanomolar to ~0.3 mM and spanning ~5−6 orders of magnitude.[2,10] One of the key issues in screening suitable Zn^{2+} probes is to design a sensing system with the Zn^{2+}-ligand dissociation contents comparable to the Zn^{2+} concentrations within cells and it is also highly desirable that the binding is reversible so that the dynamic and real-time sensing and imaging of Zn^{2+} can be achieved.[11,12]

In a further effort to understand the nature of reversible binding between Zn^{2+} ions and ZQMA moieties and to ascertain whether it is due to the thermo-induced micellization or due to the temperature effects, further experiments were conducted. PEG_{113}-*b*-P($MEO_2MA_{0.88}$-*co*-$OEGMA_{0.12}$-*co*-ZQMA)$_{60}$ with a CMT of ~39 °C can molecularly dissolve in water as unimers at 37 °C. As shown in Figure S6a in the Supporting Information, we can again observe the reversible on/off switchable fluorescence emission upon the sequential addition of Zn^{2+} ions and EDTA (~9.0-fold change). This indicates that it is elevated temperature rather than micellization-induced formation of hydrophobic microenvironments that decrease the Zn^{2+}-ZQMA binding affinity. Moreover, from Figure S6b in the Supporting Information, the detection limit of PEG_{113}-*b*-P($MEO_2MA_{0.88}$-*co*-$OEGMA_{0.12}$-*co*-ZQMA)$_{60}$ to Zn^{2+} ions was determined to be ~10 nM. This further confirmed that by modulating the OEGMA molar contents with the thermoresponsive DHBCs and the detection temperatures, the detection limits of Zn^{2+} ions can be facilely tuned.

Finally, preliminary Zn^{2+} imaging experiments within HeLa cells were further conducted. As shown in Figure 9a, HeLa cells cultured in the presence of 2.0 g/L PEG_{113}-*b*-P(MEO_2MA-*co*-ZQMA)$_{70}$ ([ZQMA] = 50.0 μM) exhibit barely discernible fluorescence emissions. When the above culture mixture was supplemented with 4.0 equiv of Zn^{2+} ions (relative to ZQMA moieties) for 30 min, a blue fluorescence emission can be clearly observed under inverted fluorescence microscopy (Figure 9b), indicating that PEG_{113}-*b*-P(MEO_2MA-*co*-ZQMA)$_{70}$ micelles can effectively enter into living cells and efficiently recognize/capture Zn^{2+} ions to afford prominently enhanced fluorescence emissions. The bright field image shown in Figure 9c revealed that the cells are still viable throughout the imaging process, implying that PEG_{113}-*b*-P(MEO_2MA-*co*-ZQMA)$_{70}$ DHBCs are almost noncytotoxic up to a concentration of 2.0 g/L. It is worthy of noting that the low cytotoxicity and biocompatible nature of PEG, $PMEO_2MA$, and POEGMA polymers has previously been reported.[96]

CONCLUSIONS

In summary, ZQMA-labeled DHBCs with the OEGMA contents varying from 0 to 12.0 mol % in the thermo-responsive block of PEG-*b*-P(MEO_2MA-*co*-OEGMA-*co*-ZQMA) were synthesized, which can serve as dual fluorescent chemosensors for temperature and Zn^{2+} ions. At 20 °C, PEG-*b*-P(MEO_2MA-*co*-ZQMA) can selectively bind Zn^{2+} ions over other common metal ions, leading to the prominent fluorescence enhancement with a detection limit down to ~3.0 nM. Upon heating above the critical micellization temperature (CMT), the fluorescence intensity of PEG-*b*-P(MEO_2MA-*co*-ZQMA) in the absence of Zn^{2+} ions exhibits a 6.0-fold increase in a narrow temperature range of 26−32 °C. Furthermore, the effective detection range of temperatures can be facilely tuned by simply varying OEGMA molar contents in the thermoresponsive block. Apart from this, reversible sensing of Zn^{2+} ions can be achieved at 37 °C, although the detection limits slightly increased to ~14 nM for PEG-*b*-P(MEO_2MA-*co*-ZQMA) and ~10 nM for PEG_{113}-*b*-P($MEO_2MA_{0.88}$-*co*-$OEGMA_{0.12}$-*co*-ZQMA)$_{60}$. In vitro fluorescence imaging studies demonstrated that the micelles can effectively enter into living cells and sensitively respond to Zn^{2+} ions. This work represents the first example of purely aqueous-based polymeric Zn^{2+} sensors by integrating the well-developed small molecule Zn^{2+}-sensing moieties with stimuli-responsive DHBCs.

ASSOCIATED CONTENT

Supporting Information. Spectroscopic/analytical data of ^1H NMR, GPC, dynamic LLS, temperature-dependent optical transmittance, and fluorescence measurements. This material is available free of charge via the Internet at http://pubs.acs.org.

AUTHOR INFORMATION

Corresponding Author
*E-mail: sliu@ustc.edu.cn.

■ ACKNOWLEDGMENT

The financial support from National Natural Scientific Foundation of China (NNSFC) Project (Grants 20874092, 91027026, and 51033005), Fundamental Research Funds for the Central Universities, and Specialized Research Fund for the Doctoral Program of Higher Education (SRFDP) is gratefully acknowledged.

■ REFERENCES

(1) Jiang, P. J.; Guo, Z. J. *Coord. Chem. Rev.* **2004**, *248*, 205–229.
(2) Frederickson, C. J.; Bush, A. I. *BioMetals* **2001**, *14*, 353–366.
(3) Koike, T.; Watanabe, T.; Aoki, S.; Kimura, E.; Shiro, M. *J. Am. Chem. Soc.* **1996**, *118*, 12696–12703.
(4) Falchuk, K. H. *Mol. Cell. Biochem.* **1998**, *188*, 41–48.
(5) Frederickson, C. J.; Koh, J. Y.; Bush, A. I. *Nat. Rev. Neurosci.* **2005**, *6*, 449–462.
(6) Ohalloran, T. V. *Science* **1993**, *261*, 715–725.
(7) Takeda, A. *BioMetals* **2001**, *14*, 343–351.
(8) Suh, S. W.; Jensen, K. B.; Jensen, M. S.; Silva, D. S.; Kesslak, P. J.; Danscher, G.; Frederickson, C. J. *Brain Res.* **2000**, *852*, 274–278.
(9) Carol, P.; Sreejith, S.; Ajayaghosh, A. *Chem.—Asian J.* **2007**, *2*, 338–348.
(10) Bush, A. I. *Curr. Opin. Chem. Biol.* **2000**, *4*, 184–191.
(11) McRae, R.; Bagchi, P.; Sumalekshmy, S.; Fahrni, C. J. *Chem. Rev.* **2009**, *109*, 4780–4827.
(12) Que, E. L.; Domaille, D. W.; Chang, C. J. *Chem. Rev.* **2008**, *108*, 1517–1549.
(13) Kim, H. N.; Guo, Z.; Zhu, W.; Yoon, J.; Tian, H. *Chem. Soc. Rev.* **2011**, *40*, 79–93.
(14) Kikuchi, K.; Komatsu, K.; Nagano, T. *Curr. Opin. Chem. Biol.* **2004**, *8*, 182–191.
(15) Terai, T.; Nagano, T. *Curr. Opin. Chem. Biol.* **2008**, *12*, 515–521.
(16) Thompson, R. B. *Curr. Opin. Chem. Biol.* **2005**, *9*, 526–532.
(17) Aoki, S.; Kaido, S.; Fujioka, H.; Kimura, E. *Inorg. Chem.* **2003**, *42*, 1023–1030.
(18) Michaels, H. A.; Murphy, C. S.; Clark, R. J.; Davidson, M. W.; Zhu, L. *Inorg. Chem.* **2010**, *49*, 4278–4287.
(19) Huang, S.; Clark, R. J.; Zhu, L. *Org. Lett.* **2007**, *9*, 4999–5002.
(20) Zapata, F.; Caballero, A.; Espinosa, A.; Tarraga, A.; Molina, P. *Org. Lett.* **2007**, *9*, 2385–2388.
(21) Sclafani, J. A.; Maranto, M. T.; Sisk, T. M.; VanArman, S. A. *Tetrahedron Lett.* **1996**, *37*, 2193–2196.
(22) Nolan, E. M.; Lippard, S. J. *Acc. Chem. Res.* **2009**, *42*, 193–203.
(23) Crivat, G.; Kikuchi, K.; Nagano, T.; Priel, T.; Hershfinkel, M.; Sekler, I.; Rosenzweig, N.; Rosenzweig, Z. *Anal. Chem.* **2006**, *78*, 5799–5804.
(24) Nolan, E. M.; Burdette, S. C.; Harvey, J. H.; Hilderbrand, S. A.; Lippard, S. J. *Inorg. Chem.* **2004**, *43*, 2624–2635.
(25) Woodroofe, C. C.; Won, A. C.; Lippard, S. J. *Inorg. Chem.* **2005**, *44*, 3112–3120.
(26) Burdette, S. C.; Frederickson, C. J.; Bu, W. M.; Lippard, S. J. *J. Am. Chem. Soc.* **2003**, *125*, 1778–1787.
(27) Burdette, S. C.; Walkup, G. K.; Spingler, B.; Tsien, R. Y.; Lippard, S. J. *J. Am. Chem. Soc.* **2001**, *123*, 7831–7841.
(28) Hirano, T.; Kikuchi, K.; Urano, Y.; Higuchi, T.; Nagano, T. *J. Am. Chem. Soc.* **2000**, *122*, 12399–12400.
(29) Hirano, T.; Kikuchi, K.; Urano, Y.; Nagano, T. *J. Am. Chem. Soc.* **2002**, *124*, 6555–6562.
(30) Komatsu, K.; Kikuchi, K.; Kojima, H.; Urano, Y.; Nagano, T. *J. Am. Chem. Soc.* **2005**, *127*, 10197–10204.
(31) Nolan, E. M.; Jaworski, J.; Okamoto, K. I.; Hayashi, Y.; Sheng, M.; Lippard, S. J. *J. Am. Chem. Soc.* **2005**, *127*, 16812–16823.
(32) Nolan, E. M.; Ryu, J. W.; Jaworski, J.; Feazell, R. P.; Sheng, M.; Lippard, S. J. *J. Am. Chem. Soc.* **2006**, *128*, 15517–15528.
(33) Tomat, E.; Nolan, E. M.; Jaworski, J.; Lippard, S. J. *J. Am. Chem. Soc.* **2008**, *130*, 15776–15777.
(34) Urano, Y.; Kamiya, M.; Kanda, K.; Ueno, T.; Hirose, K.; Nagano, T. *J. Am. Chem. Soc.* **2005**, *127*, 4888–4894.
(35) Walkup, G. K.; Burdette, S. C.; Lippard, S. J.; Tsien, R. Y. *J. Am. Chem. Soc.* **2000**, *122*, 5644–5645.
(36) Woodroofe, C. C.; Lippard, S. J. *J. Am. Chem. Soc.* **2003**, *125*, 11458–11459.
(37) Lim, N. C.; Bruckner, C. *Chem. Commun.* **2004**, 1094–1095.
(38) Lim, N. C.; Schuster, J. V.; Porto, M. C.; Tanudra, M. A.; Yao, L. L.; Freake, H. C.; Bruckner, C. *Inorg. Chem.* **2005**, *44*, 2018–2030.
(39) Mizukami, S.; Okada, S.; Kimura, S.; Kikuchi, K. *Inorg. Chem.* **2009**, *48*, 7630–7638.
(40) Li, H. Y.; Gao, S.; Xi, Z. *Inorg. Chem. Commun.* **2009**, *12*, 300–303.
(41) Komatsu, K.; Urano, Y.; Kojima, H.; Nagano, T. *J. Am. Chem. Soc.* **2007**, *129*, 13447–13454.
(42) Wu, J. S.; Liu, W. M.; Zhuang, X. Q.; Wang, F.; Wang, P. F.; Tao, S. L.; Zhang, X. H.; Wu, S. K.; Lee, S. T. *Org. Lett.* **2007**, *9*, 33–36.
(43) Hanaoka, K.; Muramatsu, Y.; Urano, Y.; Terai, T.; Nagano, T. *Chem.—Eur. J.* **2010**, *16*, 568–572.
(44) Tamanini, E.; Flavin, K.; Motevalli, M.; Piperno, S.; Gheber, L. A.; Todd, M. H.; Watkinson, M. *Inorg. Chem.* **2010**, *49*, 3789–3800.
(45) Tamanini, E.; Katewa, A.; Sedger, L. M.; Todd, M. H.; Watkinson, M. *Inorg. Chem.* **2009**, *48*, 319–324.
(46) Xu, Z. C.; Baek, K. H.; Kim, H. N.; Cui, J. N.; Qian, X. H.; Spring, D. R.; Shin, I.; Yoon, J. *J. Am. Chem. Soc.* **2010**, *132*, 601–610.
(47) Gunnlaugsson, T.; Lee, T. C.; Parkesh, R. *Org. Biomol. Chem.* **2003**, *1*, 3265–3267.
(48) Jiang, W.; Fu, Q. Q.; Fan, H. Y.; Wang, W. *Chem. Commun.* **2008**, 259–261.
(49) Qian, F.; Zhang, C. L.; Zhang, Y. M.; He, W. J.; Gao, X.; Hu, P.; Guo, Z. J. *J. Am. Chem. Soc.* **2009**, *131*, 1460–1468.
(50) Koutaka, H.; Kosuge, J.; Fukasaku, N.; Hirano, T.; Kikuchi, K.; Urano, Y.; Kojima, H.; Nagano, T. *Chem. Pharm. Bull.* **2004**, *52*, 700–703.
(51) Wu, Y. K.; Peng, X. J.; Guo, B. C.; Fan, J. L.; Zhang, Z. C.; Wang, J. Y.; Cui, A. J.; Gao, Y. L. *Org. Biomol. Chem.* **2005**, *3*, 1387–1392.
(52) Atilgan, S.; Ozdemir, T.; Akkaya, E. U. *Org. Lett.* **2008**, *10*, 4065–4067.
(53) Tang, B.; Huang, H.; Xu, K. H.; Tong, L. L.; Yang, G. W.; Liu, X.; An, L. G. *Chem. Commun.* **2006**, 3609–3611.
(54) Kiyose, K.; Kojima, H.; Urano, Y.; Nagano, T. *J. Am. Chem. Soc.* **2006**, *128*, 6548–6549.
(55) Han, Z. X.; Zhang, X. B.; Zhuo, L.; Gong, Y. J.; Wu, X. Y.; Zhen, J.; He, C. M.; Jian, L. X.; Jing, Z.; Shen, G. L.; Yu, R. Q. *Anal. Chem.* **2010**, *82*, 3108–3113.
(56) Sensi, S. L.; Ton-That, D.; Weiss, J. H.; Rothe, A.; Gee, K. R. *Cell Calcium* **2003**, *34*, 281–284.
(57) Mashraqui, S. H.; Khan, T.; Sundaram, S.; Betkar, R.; Chandiramani, M. *Chem. Lett.* **2009**, *38*, 730–731.
(58) Du, P. W.; Lippard, S. J. *Inorg. Chem.* **2010**, *49*, 10753–10755.
(59) Mahadevan, I. B.; Kimber, M. C.; Lincoln, S. F.; Tiekink, E. R. T.; Ward, A. D.; Betts, W. H.; Forbes, I. J.; Zalewski, P. D. *Aust. J. Chem.* **1996**, *49*, 561–568.
(60) Aoki, S.; Sakurama, K.; Matsuo, N.; Yamada, Y.; Takasawa, R.; Tanuma, S. I.; Shiro, M.; Takeda, K.; Kimura, E. *Chem.—Eur. J.* **2006**, *12*, 9066–9080.
(61) Aoki, S.; Sakurama, K.; Ohshima, R.; Matsuo, N.; Yamada, Y.; Takasawa, R.; Tanuma, S. I.; Talkeda, K.; Kimura, E. *Inorg. Chem.* **2008**, *47*, 2747–2754.
(62) Xue, L.; Wang, H. H.; Wang, X. J.; Jiang, H. *Inorg. Chem.* **2008**, *47*, 4310–4318.
(63) Zhou, X. Y.; Yu, B. R.; Guo, Y. L.; Tang, X. L.; Zhang, H. H.; Liu, W. S. *Inorg. Chem.* **2010**, *49*, 4002–4007.
(64) He, C. S.; Zhu, W. P.; Xu, Y. F.; Zhong, Y.; Zhou, J. A.; Qian, X. H. *J. Mater. Chem.* **2010**, *20*, 10755–10764.
(65) Frederickson, C. J.; Kasarskis, E. J.; Ringo, D.; Frederickson, R. E. *J. Neurosci. Meth.* **1987**, *20*, 91–103.
(66) Hanaoka, K.; Kikuchi, K.; Kojima, H.; Urano, Y.; Nagano, T. *J. Am. Chem. Soc.* **2004**, *126*, 12470–12476.

(67) Pearce, D. A.; Jotterand, N.; Carrico, I. S.; Imperiali, B. *J. Am. Chem. Soc.* **2001**, *123*, 5160–5161.
(68) Chen, X. Y.; Shi, J.; Li, Y. M.; Wang, F. L.; Wu, X.; Guo, Q. X.; Liu, L. *Org. Lett.* **2009**, *11*, 4426–4429.
(69) Liu, Y.; Zhang, N.; Chen, Y.; Wang, L. H. *Org. Lett.* **2007**, *9*, 315–318.
(70) Wang, H. H.; Gan, Q.; Wang, X. J.; Xue, L.; Liu, S. H.; Jiang, H. *Org. Lett.* **2007**, *9*, 4995–4998.
(71) Xue, L.; Liu, Q.; Jiang, H. *Org. Lett.* **2009**, *11*, 3454–3457.
(72) Zhang, Y.; Guo, X. F.; Si, W. X.; Jia, L. H.; Qian, X. H. *Org. Lett.* **2008**, *10*, 473–476.
(73) Bonacchi, S.; Rampazzo, E.; Montalti, M.; Prodi, L.; Zaccheroni, N.; Mancin, F.; Teolato, P. *Langmuir* **2008**, *24*, 8387–8392.
(74) Joshi, B. P.; Cho, W. M.; Kim, J.; Yoon, J.; Lee, K. H. *Bioorg. Med. Chem. Lett.* **2007**, *17*, 6425–6429.
(75) Franz, K. J.; Pearce, D. A.; Imperiali, B. *J. Inorg. Biochem.* **2001**, *86*, 222–222.
(76) Shults, M. D.; Pearce, D. A.; Imperiali, B. *J. Am. Chem. Soc.* **2003**, *125*, 10591–10597.
(77) Benson, D. E.; Wisz, M. S.; Hellinga, H. W. *Curr. Opin. Biotechnol.* **1998**, *9*, 370–376.
(78) Hellinga, H. W.; Marvin, J. S. *Trends Biotechnol.* **1998**, *16*, 183–189.
(79) Chen, Y. F.; Rosenzweig, Z. *Anal. Chem.* **2002**, *74*, 5132–5138.
(80) Ruedas-Rama, M. J.; Hall, E. A. H. *Anal. Chem.* **2008**, *80*, 8260–8268.
(81) Frederickson, C. J. *Int. Rev. Neurobiol.* **1989**, *31*, 145–238.
(82) Li, C. H.; Zhang, Y. X.; Hu, J. M.; Cheng, J. J.; Liu, S. Y. *Angew. Chem., Int. Ed.* **2010**, *49*, 5120–5124.
(83) Liu, T.; Hu, J. M.; Yin, J.; Zhang, Y. F.; Li, C. H.; Liu, S. Y. *Chem. Mater.* **2009**, *21*, 3439–3446.
(84) Li, C. H.; Liu, S. Y. *J. Mater. Chem.* **2010**, *20*, 10716–10723.
(85) Hu, J. M.; Li, C. H.; Liu, S. Y. *Langmuir* **2010**, *26*, 724–729.
(86) Wan, X. J.; Wang, D.; Liu, S. Y. *Langmuir* **2010**, *26*, 15574–15579.
(87) Yin, J.; Guan, X. F.; Wang, D.; Liu, S. Y. *Langmuir* **2009**, *25*, 11367–11374.
(88) Hu, J. M.; Liu, S. Y. *Macromolecules* **2010**, *43*, 8315–8330.
(89) van Esch, J.; Schoonbeek, F.; de Loos, M.; Kooijman, H.; Spek, A. L.; Kellogg, R. M.; Feringa, B. L. *Chem.—Eur. J.* **1999**, *5*, 937–950.
(90) Nasir, M. S.; Fahrni, C. J.; Suhy, D. A.; Kolodsick, K. J.; Singer, C. P.; O'Halloran, T. V. *J. Biol. Inorg. Chem.* **1999**, *4*, 775–783.
(91) Fahrni, C. J.; O'Halloran, T. V. *J. Am. Chem. Soc.* **1999**, *121*, 11448–11458.
(92) An, Z. S.; Tang, W.; Wu, M. H.; Jiao, Z.; Stucky, G. D. *Chem. Commun.* **2008**, 6501–6503.
(93) Han, S.; Hagiwara, M.; Ishizone, T. *Macromolecules* **2003**, *36*, 8312–8319.
(94) Lutz, J. F.; Hoth, A. *Macromolecules* **2006**, *39*, 893–896.
(95) Xu, Z. C.; Yoon, J.; Spring, D. R. *Chem. Soc. Rev.* **2010**, *39*, 1996–2006.
(96) Duncan, R. *Nat. Rev. Drug Discovery* **2003**, *2*, 347–360.